Environmental Research Letters

LETTER

Lack of cool, not warm, extremes distinguishes late 20th Century climate in 979-year Tasmanian summer temperature reconstruction

K J Allen[1,7], E R Cook[2], R Evans[3], R Francey[4], B M Buckley[2], J G Palmer[5], M J Peterson[6] and P J Baker[1]

1 School of Ecosystem and Forest Sciences, University of Melbourne, Richmond VIC 3121, Australia
2 Lamont-Doherty Earth Observatory, Palisades, NY, 10964 United States of America
3 Silviscan Pty Ltd, Doncaster East, VIC 3109, Australia
4 Oceans and Atmosphere, CSIRO, Aspendale VIC 3195, Australia
5 Climate Change Research Centre, School of Biological, Earth and Environmental Sciences, University of New South Wales, Sydney, Australia
6 351 Sheffield Rd, Acacia Hills, Tasmania, Australia
7 Author to whom any correspondence should be addressed.

E-mail: kathryn.allen@unimelb.edu.au

Keywords: Temperature reconstruction, tree-ring chronology, Australia, Tasmania, wood properties

Supplementary material for this article is available online

OPEN ACCESS

RECEIVED
5 November 2017

REVISED
18 January 2018

ACCEPTED FOR PUBLICATION
16 February 2018

PUBLISHED
15 March 2018

Abstract

Very few annually resolved millennial-length temperature reconstructions exist for the Southern Hemisphere. Here we present four 979-year reconstructions for southeastern Australia for the austral summer months of December–February. Two of the reconstructions are based on the Australian Water Availability Project dataset and two on the Berkeley Earth Surface Temperature dataset. For each climate data set, one reconstruction is based solely on *Lagarostrobos franklinii* (restricted reconstructions) while the other is based on multiple Tasmanian conifer species (unrestricted reconstructions). Each reconstruction calibrates ~50–60% of the variance in the temperature datasets depending on the number of tree-ring records available for the reconstruction. We found little difference in the temporal variability of the reconstructions, although extremes are amplified in the restricted reconstructions relative to the unrestricted reconstructions. The reconstructions highlight the occurrence of numerous individual years, especially in the 15th–17th Centuries, for which temperatures were comparable with those of the late 20th Century. The 1950–1999 period, however, stands out as the warmest 50-year period on average for the past 979 years, with a sustained shift away from relatively low mean temperatures, the length of which is unique in the 979-year record. The reconstructions are strongly and positively related to temperatures across the southeast of the Australian continent, negatively related to temperatures in the north and northeast of the continent, and uncorrelated with temperatures in the west. The lack of a strong relationship with temperatures across the continent highlights the necessity of a sub-regional focus for Australasian temperature reconstructions.

Introduction

Since 1910 Australian temperatures have increased on average by ~0.9 °C, and much of this increase has been sustained since 1970 (www.bom.gov.au). The IPCC (2012) asserts there is high confidence that, globally, temperatures will continue to rise and that hot days will become more frequent and hotter. What is less clear from instrumental data, particularly for Australia with its limited records (typically < 100 years), is whether such persistent warm conditions have occurred in previous centuries. Over the past two decades, however, significant efforts have extended the annually resolved Australasian temperature record by several hundred years (Cook *et al* 2000, 2002, PAGES 2 K Consortium 2013, Saunders *et al* 2013,

O'Donnell *et al* 2016, Gergis *et al* 2016). Without exception, these reconstructions show a strong and sustained temperature increase since at least the mid-20th Century (Cook *et al* 2000 (November–April mean temperature); Gergis *et al* 2016 (September–February mean temperature); O'Donnell *et al* 2016 (January maximum temperature); Saunders *et al* (2013, annual mean temperature)). Two of the longest reconstructions (Cook *et al* 2000, Gergis *et al* 2016) suggest recent temperatures are highly unusual in the context of the past millennium.

Despite these advances there remain critical gaps in our understanding. For example, although the Cook *et al* (2000) Mt Read warm season temperature reconstruction is based on the well-replicated and thus-far most strongly temperature-linked Australian ring-width chronology exceeding 1000 years in length, it is still based only on a single high-elevation site, and high elevation sites of *Lagarostrobos franklinii* are ecologially unusual. Would the results be the same if different species, or other sites were used? Could these better reflect temperatures across a much broader swathe of Australia? The multi-proxy continental-scale PAGES 2 K Consortium (2013) reconstructions allow broad inferences to be made, but it remains crucial to understand if and how intra-continental variability undermines the ability of a single reconstruction to represent temperatures across the entire Australasian region. Furthermore, with the important exception of O'Donnell *et al* (2016), who reconstructed maximum temperatures for a single month, none of these reconstructions have been able to capture upwards of 50% of the variance contained in the instrumental record, thus limiting confidence in inferences made from them. These considerable uncertainties underscore the pressing need for further development of climate-sensitive proxies to improve our understanding of historical climate variability and to assess current climate extremes.

Here we present four 979-year mean temperature reconstructions for the austral summer months (December–February) for southeastern Australia, a region impacted by multiple ocean-atmosphere processes including the El Niño-Southern Oscillation, the Southern Annular Mode and the Indian Ocean Dipole. The reconstructions use a network of Tasmanian tree-ring chronologies drawn from four endemic species and are a unique mix of ring-width and wood properties (see below). The availability of a large pool of potential predictors local to Tasmania provides a valuable opportunity to assess whether a Tasmanian temperature reconstruction based on multiple species and sites will substantially improve upon, or differ from, one based solely on *L. franklinii*. Skillful reconstructions also enable robust assessment of the applicability of broad geographic inferences from reconstructions based on localised reconstructions.

Methods

Climate data

We used two temperature data sets to develop our reconstructions: the highly resolved gridded Australian Water Availability Project (AWAP) mean temperature product that extends back to 1911 (0.05° × 0.05° grid; Jones *et al* 2009, Raupach *et al* 2009), and the longer but more coarsely resolved Berkeley data that extends back to 1841 (1° × 1° grid, http://berkeleyearth.org/data/, National Center for Atmospheric Research 2015). The two data sets use slightly different processes to interpolate station data. Two important differences that may affect final gridded data, especially for data sparse areas, are the lack of data homogenisation (Berkeley treats discontinuities as separate stations), and the use of data fragments of varying size (Berkeley uses fragments as short as six months whilst AWAP generally requires 12-year fragments; see Jones *et al* 2009, Rohde *et al* 2013 for details).

Because our aim was to use Tasmanian tree-ring data to reconstruct temperatures over the relatively small region of Tasmania, we sought to construct a single climate series for the entire region. However, as Tasmania is topographically heterogeneous, we first used the finely resolved Tasmanian AWAP data to determine the appropriateness of using a single temperature target for this region. We checked inter-series correlations between all possible pairs of grid cells across the region. A large proportion of low correlations between paired grid cells would suggest creation of a single target series is inappropriate. The target variable for this study is mean austral summer temperature (December–February; DJF), so anomaly series relative to the 1961–1990 reference period were created for all AWAP grid cells. Monthly data were first averaged across the three months for each grid cell in the 40–44° S and 144–149° E box to create summer mean temperature series before creating the seasonal anomaly series. This region includes the entire Tasmanian mainland as well as some of its offshore islands. All ~3.55 million pairs of grid cells were correlated at $r > 0.8$, 99% pairs of series correlated at $r > 0.85$, and 85% paired grid cells correlated at $r > 0.9$. These high correlations across the region support the creation of a single target series for Tasmania. Therefore, the DJF anomalies for all AWAP grid cells in the Tasmanian region were averaged to create a single series. The Tasmanian Berkeley data were adjusted to be relative to the 1961–1990 period. The two resultant data series are strongly correlated over their common period ($r = 0.976$; 1911–2009).

Tree-ring chronologies

All tree-ring sites are based in Tasmania, but we used two different sets of potential predictors from the available predictor pool (58 chronologies). The first network consisted of all available Tasmanian tree-ring chronologies extending up to 2009 CE and beginning at or

before 1800 CE. This set of chronologies is based on four endemic Tasmanian tree species: *L. franklinii*, *Athrotaxis selaginoides*, *Athrotaxis cupressoides* and *Phyllocladus aspleniifolius* and includes wood properties chronologies from each species. In some instances several different types of chronologies exist for a single site. For example, at the February Creek (FEB) there are nine different chronology types (table S1). This first set of predictors was used to produce what we refer to as the unrestricted reconstructions. The second set of potential predictors consists solely of *L. franklinii* chronologies that at least cover 1800–2009 CE (11 chronologies). Typically, *L. franklinii* is found along creeks and rivers at low elevations (≤400 m ASL) in western Tasmania, although it does exist above 800 m ASL (Buckley *et al* 1997, pers. obs). Buckley *et al* (1997) found strong positive relationships between warm season temperatures and the two highest elevation *L. franklinii* sites they examined, but noted that the temperature signal in low elevation tree-ring width chronologies was complex and generally weak. More recent work, however, has shown strong associations between temperature and various alternative wood properties chronologies (e.g. tracheid radial diameter (TRD), density, cell wall thickness (WT) and microfibril angle (MFA)) from low elevation sites (Allen *et al* 2013, Drew *et al* 2013). This second set of predictors therefore includes two high-elevation ring-width sites (≥800 m ASL) and *L. franklinii* wood properties chronologies from several low elevation sites (≤350 m ASL). We refer to these reconstructions as the restricted reconstructions. We use these two different networks to test whether a multi-species network provides a more reliable reconstruction of summer temperatures than one based solely on *L. franklinii* and whether using a single species has introduced systematic biases towards warmer or cooler temperatures relative to the unrestricted reconstruction.

For many of the wood properties chronologies, the number of available series was ≤60 for substantial portions of their length due to, for example, sections of the tree cores with unusable wood properties data. This meant that standardisation techniques commonly used to minimise the loss of low frequency variance but which require a large number of long, continuous samples, such as regional curve standardisation, were not suitable. In addition, nearly all tree ring sites are from mesic forest sites with complex forest dynamics such that a simple negative exponential curve/linear regression was not appropriate either. All wood properties chronologies were standardised with the Friedman super-smoother (Friedman 1984), a non-parametric detrending method in which local characteristics of the data determine the span over which data is smoothed. It is potentially more data-responsive than a cubic smoothing spline. An age-dependent spline was used to standardise the ring-width chronologies where suitable (long series lengths, majority of samples close to, or containing pith), otherwise the Friedman super-smoother was used.

The reconstructions

We used the well-documented nested principal component regression methodology (Cook *et al* 1999) to produce our reconstructions. Using this methodology, each successive group of chronologies (nest) is longer than the first but includes fewer chronologies, and each nest is individually calibrated and verified against the instrumental target. In the final reconstruction, variance of each nest is scaled to the reconstruction target to avoid artificial variability in the nested reconstruction due to differences in R^2. Only chronologies significantly correlated ($p < 0.05$; Spearman, Pearson and robust Pearson) with the target temperature series were passed to the principal components stage of the reconstruction procedure. Each nest was first calibrated against the latter part of the available temperature records (Berkeley: 1900–2009; AWAP: 1950–2009) and then verified on an earlier period (Berkeley: 1841–1899; AWAP: 1911–1949 CE). We then used the 1841–1949 (Berkeley) and 1911–1949 (AWAP) periods for calibration, and the 1950–2009 period for verification in both cases. In developing the final reconstructions, we excluded any nest (and preceding nests) that had a correlation of less than 0.5 with the most recent nest based on the greatest number of predictors. We made use of the maximum entropy bootstrap (Vinod and Lopez-de-Lacalle 2009) to produce 300 reconstructions, and report the median reconstructions in the following section. The use of the bootstrap means that interval statistics are also available for a suite of statistics commonly used to assess the quality of reconstructions. These include calibration statistics R^2 (CRSQ) and the cross-validated reduction of error for the calibration period; and verification statistics R^2 (VRSQ), reduction of error (VRE) and coefficient of efficiency (VCE). We based our assessment of whether or not the reconstructions verified on the interval estimates of VRE and VCE, rather than their point estimates as is the common practice. This means that the entire intervals of VRE and VCE need to exceed zero for a reconstruction to be considered skillful.

Results

Chronologies selected for use in the two sets of reconstructions are shown in figure 1 and table S1. Whereas the restricted reconstructions rely solely on west Tasmanian chronologies, the unrestricted reconstructions also include chronologies in the south and central north. Substantial overlap exists between the chronologies used in the restricted and unrestricted AWAP and Berkeley reconstructions. The wood properties chronologies, especially TRD, MFA and WT, are relatively strongly correlated with temperature and add significant value to the new reconstructions

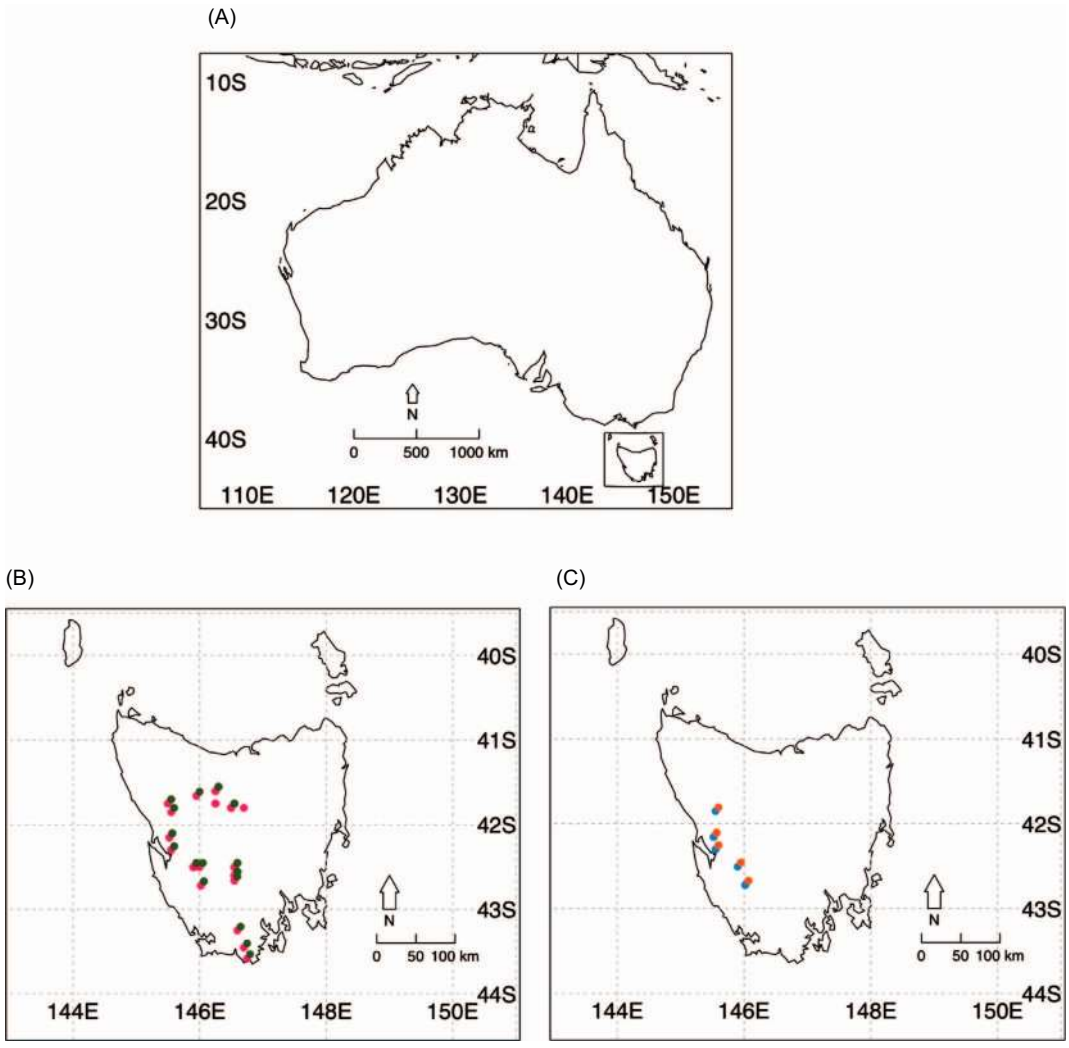

Figure 1. Sites used in the four reconstructions. (*A*) Map of Australia showing location of Tasmania. (*B*) Unrestricted reconstructions. Sites used in the AWAP reconstruction are green and those used in Berkeley reconstruction are pink. (*C*) Restricted reconstructions. Orange represents sites used in the AWAP reconstruction and blue, those used in the Berkeley reconstruction. See table S1 for site names and chronologies.

(tables S21 and S2). For the restricted reconstructions, MFA ($n = 1$) and TRD ($n = 3$) are most strongly correlated, on average, with the AWAP target while ring-width ($n = 2$) is most strongly correlated with the Berkeley target (table S2). In the unrestricted reconstructions, strongest average correlation with temperature occurs for *L. franklinii* RW in both cases if only those types with >1 chronology are considered (table S2). *Lagarostrobos franklinii* TRD (*A. selaginoides* RW) is most heavily weighted, on average, in the unrestricted Berkeley (AWAP) reconstructions. *L. franklinii* TRD is most heavily weighted, on average, for both restricted reconstructions. *L. franklinii* chronologies were most likely species, and WT chronologies the most likely wood property, to pass initial correlation screening. Conversely, *P. aspleniifolius* and ring-width chronologies were the most likely species and property type respectively to fail screening (table S1; unrestricted reconstructions).

The restricted reconstructions are comprised of three nests while the unrestricted reconstructions consist of 16 (AWAP) or 17 (Berkeley) nests. Three of the four reconstructions verify back to 1030 CE (figures 2(*k*)–(*n*)), while the unrestricted Berkeley reconstruction verifies back to 1520 CE, with a brief exception ~1700 CE. Calibrated variance (CRSQ) in the most recent nest is ~60% for all reconstructions, with a VRSQ of ~44% (figure 2(*a*)–(*d*)). Even in the earlier nests of three reconstructions, ~50% of variance is calibrated and 30%–40% is verified (figures 2(*e*)–(*j*)). The AWAP and Berkeley reconstruction models based on early calibration periods (Berkeley: 1841–1950; AWAP: 1911–1949) suggest temporal stability of the relationship between the target temperature and reconstructions, regardless of calibration interval used (figure S1). Notably however, the temperatures since 2004 years are underestimated in all cases (figures 2(*a*)–(*d*)), the biggest departures occurring for the AWAP reconstructions. The interval estimates of the calibration and verification statistics are consistently narrower for the Berkeley reconstructions. Prior to 1500 CE, verification statistics are stronger for the AWAP than the Berkeley

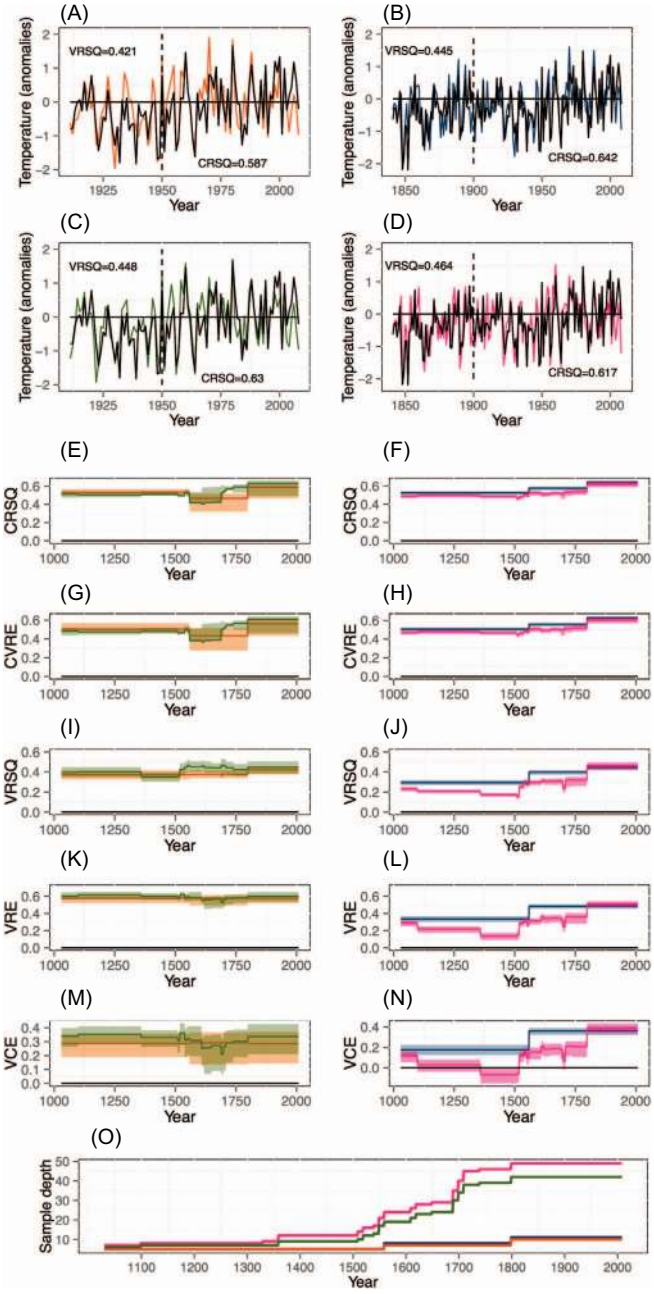

Figure 2. (*A*)−(*D*) Comparison of each reconstruction and the instrumental target over the instrumental period. Black series in (*A*)−(*D*) are the instrumental mean DJF targets. Blue is the restricted Berkeley reconstruction, pink the unrestricted Berkeley reconstruction, orange the restricted AWAP reconstruction and green the unrestricted AWAP reconstruction. Also shown is variance explained in the calibration and verification periods. (*E*)–(*N*) Calibration and verification statistics for all nests (see text). Colours as for (*A*−*D*). (*O*) Sample depth of the respective reconstructions over time. Note that the interval estimates of the statistics do not show a monotonic decrease back in time for either of the AWAP reconstructions, or for the unrestricted Berkeley reconstruction.

reconstructions, but VRSQ and VCE are comparable after 1500 CE (figures 2(*m*)−(*n*)). The point estimates of VRE are noticeably higher for the AWAP reconstructions, but the narrower bootstrapped intervals for the restricted Berkeley VCE make it comparable to VCE for the two AWAP reconstructions after 1500 CE. Lowest VCE (also VRE) values occur from 1600–1800 CE in the unrestricted AWAP reconstruction, a period when there was a rapid increase in the number of chronologies included in these reconstructions (figure 2(*o*)). This period is also wholly within the period during which the unrestricted Berkeley reconstruction fails to verify. The wider and generally lower interval estimates of the statistics for the unrestricted Berkeley reconstruction relative to the restricted Berkeley reconstruction (figures 2(*f*, *h*, *j*, *l*, *n*)) reveal its poorer quality. Interval estimates of the statistics for the two AWAP reconstructions overlap most of the time, suggesting no substantive difference in the quality of the two AWAP reconstructions (figures 2(*e*, *g*, *i*, *k*, *m*)).

Despite these differences, all four reconstructions show very similar temporal variability (figures 3(*a*)−(*f*)) and are highly correlated with one another

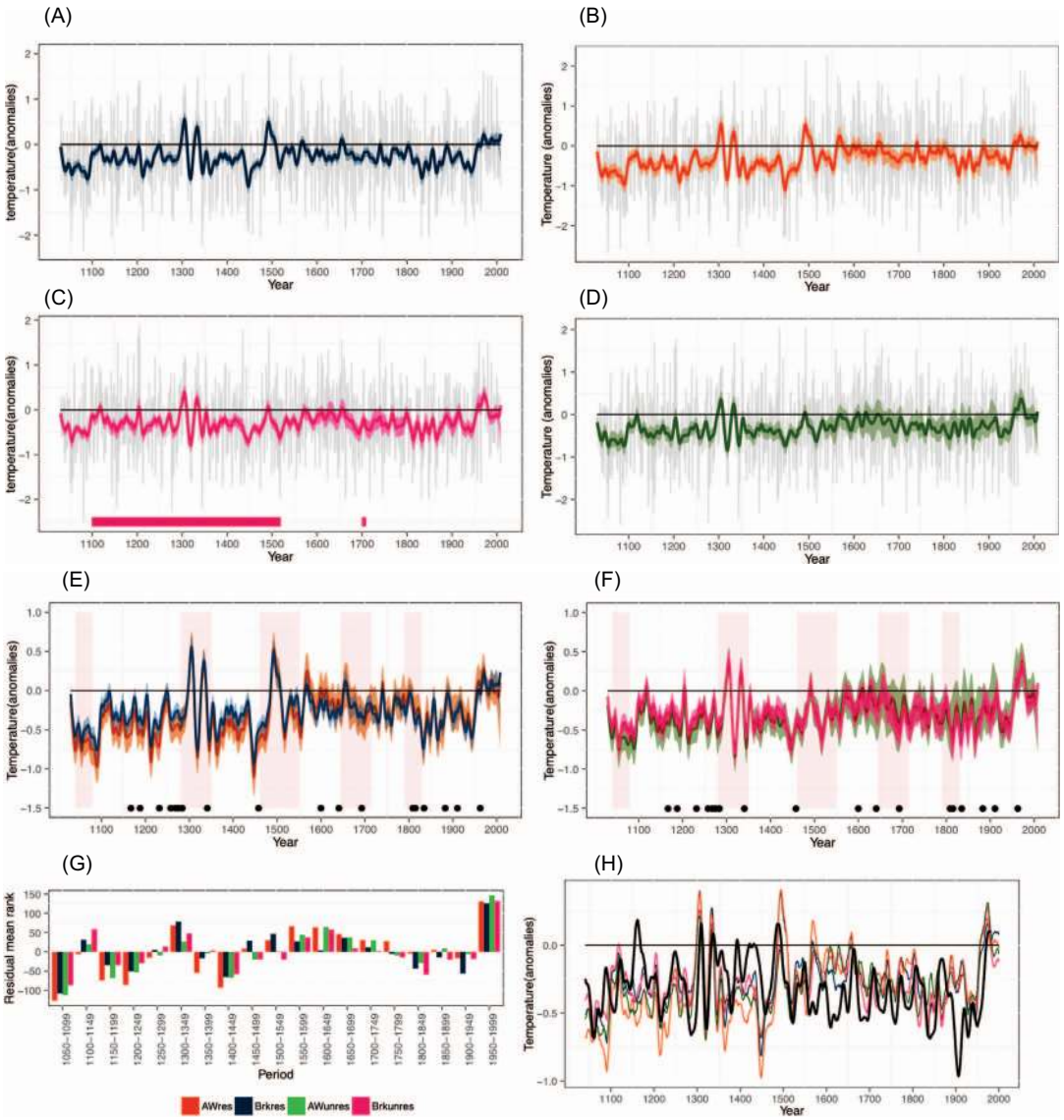

Figure 3. The AWAP and Berkeley reconstructions for Tasmania. (*A*) (Berkeley) and (*B*) (AWAP) restricted reconstructions. (*C*) (Berkeley) and (*D*) (AWAP) unrestricted reconstructions. Interannual reconstructions in grey, 20-year spline smoothed reconstructions in colour (colours as for figure 2). (*E*) Comparison of smoothed restricted Berkeley (blue) and AWAP (orange) restricted reconstructions. (*F*) Comparison of smoothed unrestricted Berkeley (pink) and AWAP (olive green) reconstructions. Pink bars are solar minima and black dots represent volcanic eruptions in which ≥ 10 Tg sulphur was emitted into atmosphere. Thick horizontal bar (*C*) indicates period for which interval estimate of VCE < 0, indicating a lack of skill. Note the relatively narrow intervals for both the Berkeley reconstructions. All reconstructions contain the same general features, but the ~1500CE peak is muted in the unrestricted reconstructions. (*G*) Difference between mean rank of defined 50-year periods of each reconstruction and overall mean rank for 1050–1999 of same reconstruction. (*H*) Comparison of the smoothed Cook *et al* (2000) November–April reconstruction (black) with the new smoothed restricted and unrestricted December–February reconstructions (colours as per figure 2).

($r > 0.8$; table S4). The general pattern is one in which temperatures were lowest for a sustained period from 1030–1100 CE, a short period ~1450 CE and highest for short periods ~1300, 1320 and 1500 CE. The longest sustained period of relatively high temperatures in the reconstructions is the post 1950 CE period although there are clearly individual years much earlier that were warmer than any in the post-1950 period (figures 3(*a*)–(*f*)). Based on the average rank for successive non-overlapping 50-year periods, the 1950–1999 period is unequivocally the warmest 50-year period in the reconstructions and the 1050–1100 CE period, the coolest (figure 3(*g*)). This result is strongly linked to fewer summers with low mean summer temperatures since 1950 (figures 3(*a*)–(*d*)). All four reconstructions suggest the 1400–1449 CE and the 1150–1249 CE 50-year periods were also relatively cool and 1300–1349 CE and 1550–1699 CE were relatively warm (figure 3(*g*)). With respect to individual years, there is considerable overlap in the top ten warmest or coolest years amongst the reconstructions (table 1), and five of these-three cool (1081, 1144 and 1344) and two warm (1493 and 1980)-are common across all reconstructions.

While the four reconstructions are very similar to one another, there are also some notable differences amongst them. Although the Berkeley reconstructions suggest slightly warmer temperatures from

Table 1. Ten most extreme cool and warm events in the four reconstructions (most extreme at the top of each list). Large bold italics indicate a year in the top ten that occurs in all four reconstructions. There are three such cool (1081, 1144 and 1344) and two warm (1493 and 1980) events. Small italics indicate a year that occurs in the top ten for one reconstruction only. The years 1832 and 1848 (cool) occur in the top ten only for the two Berkeley reconstructions; 1840 is in the top ten warm events for the two AWAP reconstructions; 1448, 1457, 1474 (cool) and 1541, 1565, 1610, 1970 (warm) occur in the top ten only in the restricted reconstructions; 1155, 1277, 1663 and 1717 (cool) and 1157, 1205, 1625 and 1960 (warm) are all in the top ten events in the two unrestricted reconstructions.

Coolest			
Berkeley restricted	Berkeley unrestricted	AWAP restricted	AWAP unrestricted
1081	*1081*	1054	*1081*
1344	1277	1745	1277
1054	*1344*	*1081*	*1344*
1474	1155	*1344*	1054
1144	1717	*1144*	*1390*
1745	1663	1474	1717
1832	*1518*	1457	1155
1848	1848	*1444*	*1144*
1457	1832	1448	1663
1448	*1144*	*1280*	1745
Warmest			
Berkeley restricted	Berkeley unrestricted	AWAP restricted	AWAP unrestricted
1493	1205	1541	1435
1541	*1493*	*1493*	*1493*
1655	1435	1970	1625
1970	*1202*	*1980*	1205
1435	1739	*1789*	*1980*
1988	1655	1565	1157
1980	1960	1840	*1335*
1335	1157	1739	*1662*
1610	*1980*	1655	1840
1565	1625	1610	1960

~1030–1450 CE and again after ~1950 than the AWAP reconstructions, the overlapping bootstrapped intervals of the smoothed reconstructions indicate these differences are almost never significant ($p < 0.1$; figure 3(*e*)–(*f*)). The bootstrapped interval estimates are noticeably wider for the unrestricted reconstructions (figure 3(*f*)), especially from 1550–1750 CE with the rapid increase in the number of chronologies included. Likewise, the intervals for both AWAP reconstructions are wider than their Berkeley counterparts (figures 3(*e*)–(*f*)). One important difference amongst the reconstructions is the greater expression of the warmest and coolest anomalies in the restricted reconstructions (e.g. 1450 (cool) and 1500 (warm)), particularly prior to 1600 CE (figures 3(*a*)–(*f*)). These likely reflect the greater sensitivity of *L. franklinii* to climate extrema relative to the other species. However, they may also reflect the smaller number of chronologies in the restricted reconstructions. Nevertheless, the fact that variance explained by the reconstructions decreases only marginally when a sizable number of predictors is removed from the predictor pool suggests that the restricted data set captures the majority of variability very well, while several predictors add little value (figures 2 and 3, table S1).

Frequency domain characteristics of the reconstructions are briefly discussed in the supplementary material (figure S2) available at stacks.iop.org/ERL/13/034041/mmedia.

Discussion

At a global scale, composites of thermally sensitive records suggest a prolonged decline in temperatures since ~1000 CE (PAGES 2 K Consortium 2017) until the increase over the past century over so. Two of three sets of land-based temperature proxies (tree rings and lake sediments), however, suggest an hiatus in this trend ~1500–1600 CE (PAGES 2 K Consortium 2017), a period that overlaps with a relatively warm period in the Tasmanian reconstructions (figure 3). The PAGES 2 K tree-ring composite also shows a sharp decline ~1450–1500 CE, coincident with the very cool period shown in our reconstruction. After ~1500 CE, both our reconstructions and the PAGES 2 K tree-ring and lake sediment composites indicate relatively low temperatures until the late 19th (PAGES 2 K Consortium 2017) or mid-20th Centuries (our reconstructions).

Only two other annual multi-month warm season temperature reconstructions covering Tasmania exist. The Gergis *et al* (2016) September–February reconstructions used a single temperature target for all of Australaisa (0–50°S, 110–180°E). As the relationship between continental Australian temperatures and Tasmanian temperatures is weak ($r \sim 0.25$; Berkeley data, figure S3), the comparison of our Tasmanian reconstructions and the Gergis *et al* (2016) reconstructions seems unwarranted here. Although the seasonal targets differ for our new reconstructions and the Cook *et al* (2000) November–April reconstruction, both reconstructions are for Tasmania only, so comparison with our reconstructions seems reasonable. Despite the different windows and greater number of proxies in our new reconstructions, they compare moderately well with the Mt Read reconstruction (mean $r = 0.53$). Our new reconstructions represent a significant improvement on this reconstruction, explaining ~60% (~44%) of the variance in the calibration (verification) period, whereas the Cook *et al* (2000) reconstruction explains 47% (~27%) in the calibration (verification) periods. There are also some important differences between our reconstructions and the previous Mt Read reconstruction that depicted the recent increase in warm season mean temperatures as a relatively monotonic trend from the early-mid 20th Century. This compares with a step-like change from the mid-20th Century in our reconstructions (especially the restricted reconstructions). Anomalies in our reconstructions are more negative than those in the Cook *et al* (2000) reconstruction for the periods ~1080–1200 CE and ~1350–1450 CE. Additionally, differences between the previous Mt Read and the new reconstructions and

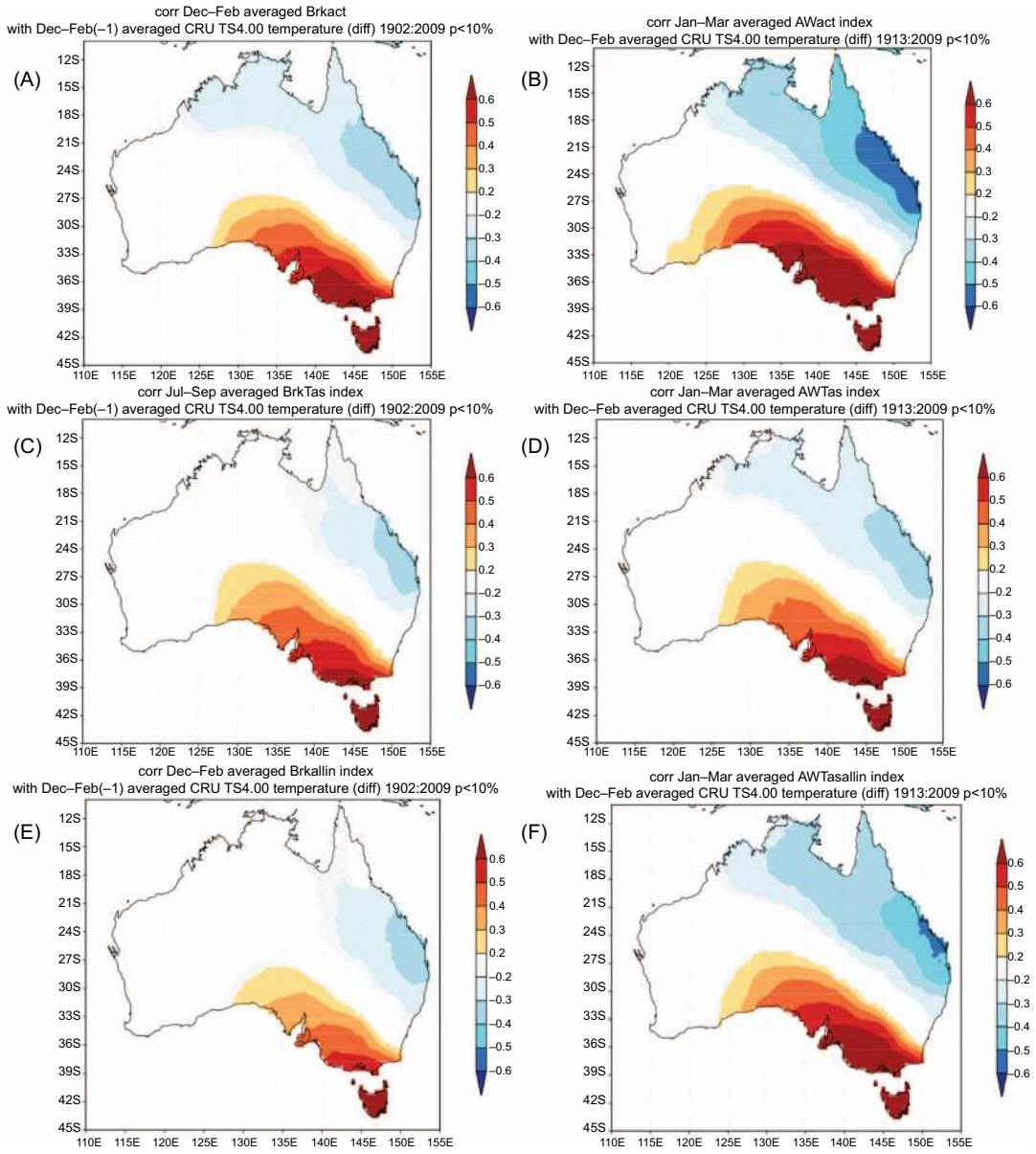

Figure 4. Comparison of instrumental targets and reconstructions with CRU 4.0 temperatures for Australia. (*A*) and (*B*) 'instrumental' target series for Tasmania and CRU4.0 for Australia; (*C*) and (*D*) restricted reconstructions and CRU 4.0, (*E*) and (*F*) unrestricted reconstructions and CRU 4.0. Left column is Berkeley data/reconstructions, right column is AWAP data/reconstructions.

at 1550–1650 CE and at ~1900 CE stand out (figure 3(*h*)). Notably, the extremity of the temperature peaks and troughs at ~1300, 1320, 1450 and 1500 CE in our unrestricted reconstructions are of similar magnitude to those in the Mt Read reconstruction.

While the amount of variance captured by our reconstructions, and the verification statistics, are impressive for this region, it remains important to assess the domain over which inferences made from them are likely to be applicable. This is particularly relevant when our reconstructions are based on temperature proxies from a relatively small area of southern Australia. We therefore used the gridded CRUTS3.24.01 data (KMNI Explorer: http://climexp.knmi.nl/) to examine this. The Tasmanian Berkeley temperature series is strongly and positively related to CRU temperatures across much of southeastern Australia, especially Tasmania and the south of mainland Australia ($r > 0.6$; figure 4). It is moderately and negatively correlated with temperatures along the eastern Queensland coast, and has a weak negative association with temperatures in the far north but no relationship with temperatures in the west. The Tasmanian AWAP data series has a much stronger negative relationship with temperature along the northeast Australian coast and stronger positive correlations across the southeast than does the Tasmanian Berkeley data (figure 4), but like the Berkeley data, is not related to temperatures in Western Australia. Queensland's location in the south-easterly trades zone and Tasmania's in the westerly wind belt will affect synoptic systems over the regions. The summertime southward extension of the Intertropical Convergence Zone will enhance periodic cyclogenesis, producing lower temperatures over Queensland.

Meanwhile, summer conditions in Tasmania are typically associated with stable air masses commonly linked to the summertime southward expansion or intensification of the subtropical ridge. More specifically, very hot conditions in the southeast are generally related to a blocking high-pressure cell in the Tasman Sea to the east that also enhances easterly flow over Queensland, leading to cooler conditions there.

The relationships between the actual temperature data are a gauge of the strength of the reconstructions. The two Berkeley reconstructions (especially the restricted Berkeley) capture the relationship across southeastern Australia, the negative relationship with coastal Queensland temperatures and the lack of any relationship with temperatures in the west, yet fail to capture the negative association with temperatures in the far north. In contrast, the unrestricted AWAP reconstruction better captures the relationship between the Tasmanian AWAP series and temperatures across Australia than does the restricted AWAP reconstruction. The strong similarity of patterns in figures 4(*c*)−(*f*) to those in 4(*a*)−(*b*) confirms that all four reconstructions reflect the spatial relationships observed in the gridded climate data for the 20th Century. While our results indicate it is reasonable to make inferences about past temperature variability for southeastern Australia based on our reconstructions, it would be inappropriate to use them to infer the temperature history of western Australia. The modest inverse correlations between the Tasmanian reconstructions and northern/northeastern temperatures suggest that some southern temperature proxies may prove useful ancillary predictors for temperature reconstructions in northern Australia, but they should not be used as primary predictors for northern temperatures. Primary predictors should instead be local.

The impact of natural external forcing such as solar variability and volcanic eruptions on climate variability is of increasing interest (e.g. Atwood *et al* 2016, Otto-Bliesner *et al* 2016, Rao *et al* 2017, Cook *et al* 2007, Anchukaitis *et al* 2017, Tejedor *et al* 2017). Solar variability has been found to coincide with low-growth periods in Northern Hemisphere trees (e.g. Büntgen *et al* 2006, Anchukaitis *et al* 2013, 2017). With perhaps the exception of the Oort minimum ∼1040−80 CE, however, there is no clear correspondence between solar minima and generally cool periods in our Tasmanian reconstructions (figures 3(*e*)−(*f*)). A key finding in relation to volcanic forcing has been that the effects of eruptions are spatially heterogeneous (Anchukaitis *et al* 2017, Guillet *et al* 2017). A visual inspection of figures 3(*e*)−(*f*), indicates little consistency between cool reconstructed conditions and large volcanic eruptions in the Southern Hemisphere (Gao *et al* 2008, Cole-Dai *et al* 2013). This lack of correspondence was confirmed by three different superposed epoch analyses based on volcanic eruptions leading to ≥10 Tg, ≥20 Tg and ≥50 Tg respectively, of sulphate aerosols in the Southern Hemisphere atmosphere (Package dplR; Bunn 2008). The dominance of an oceanic signal in Tasmanian climate may be responsible for both the lack of a volcanic signal in our reconstructions and the rather different expression of increased temperatures in the latter part of the 20th Century compared to the Australian mainland and, more generally, the Southern Hemisphere (figure S3). These differences also play out in CMIP ensemble projections (from the KMNI Climate Change Atlas) where the mean trajectory of projections for Tasmania out to ∼2050 CE are flatter than those for Australia as a whole (figure S4). These variations in historical as well as modeled projections further highlight the importance of subregional temperature reconstructions in the Australian region.

Conclusions

The reconstructions presented here are amongst the longest verified annual mean temperature reconstructions for the Southern Hemisphere, and their strength depends heavily on novel wood properties chronologies. Calibrated variance and reconstruction skill are higher than previous mean temperature reconstructions for southeastern Australia. Although the warmest summers of the post-1950 CE period are not unprecedented in the past millennium, the near complete absence of relatively cool summers is unique to last 50 years of the 20th Century. Temperature extremes in the new reconstructions are temporally consistent with those in a previous Tasmanian temperature reconstruction but are much more pronounced in the two restricted reconstructions shown here, pointing to the greater sensitivity of *L. franklinii* wood properties to both high and low temperatures. This greater emphasis on extremes is the main point of difference between the unrestricted and restricted reconstructions, and demonstrates that little information is sacrificed through the use of the restricted predictor set in this case. The results are particularly encouraging for the development of much longer temperature reconstructions from this part of the world based solely on well-preserved subfossil *L. franklinii*. Our results also firmly indicate that greater emphasis on subcontinental reconstructions for Australasia is required in order to furnish further insights into regional temperature variability across Australia over long time scales.

Acknowledgments

We thank Scott Nichols for technical assistance in developing the chronologies, Greg Lee for computing assistance, and Carly Tozer, James Risbey, Didier Monselesan, Michael Grose and Ben Cook for useful discussions about this work. We thank Parks Tasmania, ForestryTas and Hydro Tasmania for

permission to access sites. The work was supported by Australian Research Council grants DP1201040320 and DP15010325 to PJB and ERC and FT120100715 to PJB. It is Lamont-Doherty contribution no. 8195. We also thank two reviewers for their constructive comments that have helped improve this work. Reconstructions presented in this article are available from the corresponding author.

ORCID iDs

K J Allen https://orcid.org/0000-0002-8403-4552

References

Allen K J, Drew D M, Downes G M, Evans R, Cook E R, Battaglia M and Baker P J 2013 A strong regional signal in low elevation Huon pine *J. Quatern. Sci.* **28** 433–8

Anchukaitis K J, D'Arrigo R D, Andreu-Hayles L, Frank D, Verstege A, Curtis A, Buckley B M, Jacoby G C and Cook E R 2013 Tree-ring reconstructed summer temperatures from northwestern North America during the last nine centuries *J. Clim.* **26** 3001–12

Anchukaitis K J *et al* 2017 Last millennium Northern Hemisphere summer temperatures from tree rings: Part II, spatially resolved reconstructions *Quatern. Sci. Rev.* **163** 1–22

Atwood A R, Wu E, Frierson D M W, Battisti D S and Sachs J P 2016 Quantifying climate forcings and feedbacks over the last millennium in the CMIP5 P MIP3 models *J. Clim.* **29** 1161–78

Buckley B M, Cook E R, Peterson M J and Barbetti M 1997 A changing temperature response with elevation for Lagarostrobos franklinii in Tasmania, Australia *Clim. Change* **36** 477–98

Bunn A G 2008 A dendrochronology program library in R (dplR) *Dendrochronologia* **26** 115–24

Büntgen U, Frank D, Wilson R, Carrer M, Urbinati C and Esper J 2006 Testing for tree-ring divergence in the European Alps *Glob. Change Biol.* **14** 2443–53

Cook E R, Meko D M, Stahle D W and Cleaveland M K 1999 Drought reconstruction for the continental United States *J. Clim.* **12** 1145–62

Cook E R, Buckley B M, D'Arrigo R D and Peterson M J 2000 Warm-season temperatures since 1600 BC reconstructed from Tasmanian tree rings and their relationship to large-scale sea surface temperature anomalies *Clim. Dyn.* **16** 79–91

Cook E R, Palmer J G, Cook B I, Hogg A and D'Arrigo R D 2002 A multi-millennial palaeoclimatic resource from *Lagarostrobos colensoi* tree-rings at Oroko Swamp, New Zealand *Glob. Planet. Change* **33** 209–20

Cook E R, Seager R, Cane M A and Stahle D W 2007 North American drought: reconstructions, causes and consequences *Earth Sci. Rev.* **81** 93–134

Cole-Dai J, Ferris D G, Lanciki A L, Savarino J, Thiemens M H and McConnell J R 2013 Two likely stratospheric eruptions in the 1450s C.E. found in a bipolar, subannually dated 800 year ice core record *J. Geophys. Res.: Atmos.* **118** 7459–66

Drew D M, Allen K J, Downes G M, Evans R, Battaglia M and Baker P J 2013 Wood properties in a long–lived conifer reveal strong climate signals where ring width series do not *Tree Physiol.* **33** 37–47

Friedman J H 1984 A variable span scatterplot smoother *Standford University Technical Report* No. 5

Gao C, Robock A and Ammann C 2008 Volcanic forcing of climate over the past 1500 years: an improved ice core-based index for climate models *J. Geophys. Res.* **113** D23111

Gergis J, Neukom R, Gallant A J E and Karoly D J 2016 Australasian temperature reconstructions spanning the last millennium *J. Clim.* **29** 5365–92

Guillet S *et al* 2017 Climate response to the samalas volcanic eruption in 1257 revealed by proxy records *Nat. Geosci.* **10** 123–8

IPCC 2012 *Managing the Risks of Extreme Events and Disasters to Advance Climate Change Adaptation. A Special Report of Working Groups I and II of the Intergovernmental Panel on Climate Change* ed C B Field *et al* (Cambridge: Cambridge University Press) p 582

Jones D, Wang W and Fawcet R 2009 High-quality spatial climate data sets for Australia *Aust. Meteorol. Oceanogr. J.* **58** 233–48

National Center for Atmospheric Research 2015 The Climate Data Guide: Global surface temperatures: BEST: Berkeley Earth Surface Temperatures (https://climatedataguide.ucar.edu/climate-data/global-surface-temperatures-best-berkeley-earth-surface-temperatures)

O'Donnell A J, Allen K J, Evans R M, Cook E R, Trouet V and Baker P J 2016 Wood density provides new opportunities for reconstructing past temperature variability from southeastern Australian trees *Glob. Planet. Change* **141** 1–11

Otto-Bliesner B L, Brady E C, Fasullo J, Jahn A, Landrum L, Stevenson S, Rosenbloom N, Mai A and Strand G 2016 Climate variability and change since 850CE: an ensemble approach with the community earth system model *Bull. Am. Meteorol. Soc.* **97** 735–54

PAGES 2 K Consortium 2013 Continental-scale temperature variability during the past two millennia *Nat. Geosci.*

PAGES 2 K Consortium 2017 A global multiproxy database for temperature reconstructions of the Common Era *Sci. Data* **4** 170088

Rao M P *et al* 2017 European and mediterranean hydroclimate responses to tropical volcanic forcing over the last millennium *Geophys. Res. Lett.* **44** 5104–12

Raupach M R, Briggs P R, Haverd V, King E A, Paget M and Trudinger C M 2009 Australian water availability project (AWAP): CSIRO marine and atmospheric research component: Final Report for Phase 3 *CAWCR Technical Report* No. 013. p 67

Rohde R, Muller R, Jacobsen R, Perlmutter S, Rosenfeld A, Wurtele J, Curry J, Wickham C and Mosher S 2013 Berkeley earth temperature averaging process *Geoinformatics and Geostatistics: An Overview* **1** 2

Saunders K M, Grosjean M and Hodgson D A 2013 A 950 yr temperature reconstruction from Duckhole Lake, southern Tasmania, Australia *Holocene* **23** 771–83

Tejedor E, Saz M A, Cuadrat J M, Esper J and de Luis M 2017 Temperature variability in the iberian range since 1602 inferred from tree-ring records *Clim. Past* **13** 93–105

Vinod H D and Lopez-de-Lacalle J 2009 Maximum entropy bootstrap for time series: the meboot R package *J. Stat. Soft.* **29** 1–19